Investigation and in Vitro Bioactivity Study of Prepared Nanostructured Bioactive Glass

Alshimaa Ali
Department of physics, Faculty of Science, Menofia University, Egypt

Manar M. Ahmed
Department of Glass Research, National Research Center, Cairo, Egypt

L.M Sharaf El-Deen
Department of physics, Faculty of Science, Menofia University, Egypt

M.M. Elkholy
Department of physics, Faculty of Science, Menofia University, Egypt

B. M. Abd El Hady
Department of Polymers and Pigments, National Research Center, Cairo, Egypt

Abstract- In the present study nanostructured bioactive glass was synthesized via sol–gel technique. The obtained powder was characterized using several techniques: [X-ray diffraction (XRD), Fourier transform infrared spectrometer (FTIR), scanning electron microscopy (SEM), energy dispersive X-ray (EDX) and transmission electron microscope (TEM)]. The specific surface area and mean pore size of the calcined bioactive glass powders were investigated by nitrogen (N_2) adsorption and desorption isotherm. In vitro bioactivity of the prepared system was tested by immersion it in simulated body fluid (SBF). EDX and FTIR and SEM techniques were done also after soaking in SBF to confirm the hydroxycarbonate apatite (HCA) layer formation or not. The results showed that the formation of hydroxycarbonate apatite (HCA) layer on the sample surface, approving the considerable bioactivity of prepared glass powder.

Keywords – Bioactive glass, Sol–gel, Hydroxycarbonate apatite.

I. INTRODUCTION

Recently, bioactive glass (BG) represent one of the most successful bioceramic for repairing and regeneration of bone tissues [1]. The possible applications of bioactive glasses have been expanded into soft tissue repair applications particularly in wound healing [2, 3]. Larry Hench invented the first bioactive glass which contains 46.1 mol.% SiO_2, 24.4 mol.% Na_2O, 26.9mol.% CaO and 2.6 mol.% P_2O_5 [4]. The bioactivity of this glass was achieved with the formation of hydroxycarbonate apatite (HCA) layer upon immersion in physiological fluid [5]. For silicate bioactive glasses, there are various reactions that occur to form HCA layer. These reactions are cations exchange with hydrogen ions from the surrounding solution; surface glass dissolution and silica network breakdown; formation of silanols bonds at the glass solution interface; formation of a rich silica layer; migration of Ca^{2+} and PO_4^{3-} to the surface through the SiO_2-rich layer, the formation of a Ca-P layer and crystallization this layer to form HCA [6, 7]. A lot of studies have been done on bioactive glasses due to their good bioactivity, osteoconductivity and biodegradability [8– 10].

Bioactive glasses can be produced by the traditional melting route or by sol-gel process [4, 11, 12]. Sol-gel method has advantages over traditional melt method due to its lower processing temperature, presence of porosity and homogeneity and the better control on composition [12- 14]. Moreover, bioactivity of sol-gel glass can be controlled not only by the composition, but also by the process in itself [15, 16].

Li et al. presented that CaO-P_2O_5-SiO_2 powders formed by sol-gel method had bioactivity better than the melt-derived glasses of the identical composition [14]. The properties of bioactive glasses depend strongly on the compositional range [17].

The nanostructured bioactive glass present high specific surface area and are biocompatible. Therefore, nanostructured bioactive glass formed via sol-gel method are good applicant to be carriers for drug delivery [15]. By joining sol-gel and surfactant supramolecular chemistries, it is possible to acquire ordered mesopore structures, giving a higher specific surface area [15, 18, 19].

In the present work, we prepared a nanostructured bioactive glass composed of 52 wt.% SiO_2, 41 wt.% CaO, 7 wt.% P_2O_5 via sol –gel method. Structure and bioactivity of prepared sample were investigated using various techniques: (XRD), (FTIR), (TEM), (SEM) and (EDX). Also, the specific surface area and mean pore size of the prepared glass powders were examined by N_2 adsorption and desorption isotherm.

II. MATERIALS AND METHOD

2.1 Materials

Tetraethyl orthosilicate (TEOS, Merk), calcium nitrate tetrahydrate (Ca $(NO_3)_2.4H_2O$, LOBA) and triethyl phosphate (TEP, Fluka) with purification ⩾98% were used as starting materials to prepare bioactive glass powder for the present study. Absolute ethanol (C_2H_5OH, Merk), 33% ammonia solution (NH_4OH, Merk) and 68% nitric acid (HNO_3, Merk).

2.2. Sol-gel synthesis

Bioactive glass powder composed of [52% SiO_2, 41% CaO, 7% P_2O_5] in wt. % was synthesized via a quick alkali-mediated sol– gel method [20, 21]. For the preparation, firstly TEOS, distilled water, 2 M nitric acid (as a hydrolysis catalyst), were consecutively mixed in absolute ethanol at room temperature. The mixture was stirred well for 1 hour. Then for each compound: (TEP), Ca $(NO_3)_2.4H_2O$) was added respectively under magnetic stirring at room temperature. After the last addition, the mixture was kept under continuous stirring for 1 hour to facilitate hydrolysis reaction to complete. Then, 2 M ammonia solution (a gelation catalyst) was dropped into the resulting transparent solution during vigorous stirring. The final solution was swiftly gelated. The resulted gel was moved into a conventional ultrasonic bath to prevent the formation of a bulk gel. Finally, the obtained gel was kept in the drying oven at 75 °C for 3 days. The dry gel powder was heated at 650 °C for 2 hours (3 °C /min) to stabilize the glass and remove the residual nitrate. Then, the stabilized glass was ground and sieved.

2.3 Preparation of SBF

The SBF was prepared by dissolving NaCl, KCl, $K_2HPO_4.3H_2O$, $MgCl_2.6H_2O$, $CaCl_2$, and Na_2SO_4 in distilled according to the formula proposed by Kokubo et al. [22]. The solution was buffered at pH 7.4 with tris (hydroxymethyl) aminomethane and 1M HCl at 37 ^{0}C. The SBF ion concentration (mM/litre) were Na^+ 142.0, K^+ 5.0, Ca^{2+} 2.5, Mg^{2+} 1.5 HCO_3^- 4.2 Cl^- 148 HPO_4^{2-} 1.0, SO_4^{2-} 0.5. The mentioned Ion concentration of SBF analogous to those of the human plasma.

2.4 Characterization of nano-bioactive-glass

The powder X-ray diffraction (XRD) pattern was recorded using GNR X-ray diffractometer, APD 2000 PRO Model, with Cu-$K_{\alpha 1}$ radiation (λ= 1.54056 Å). The morphology and particle size of the calcined bioactive glass powder were characterized by TEM (JEM-2100 model) working at 200 kV. The infrared absorption spectra of the calcined bioglass powders before and after immersion in SBF were recorded using FTIR spectrometer, Tensor 27 Model, in 400–4000 cm^{-1} range. The composition and surface morphology of bioactive glass disks before and after soaking in SBF were analyzed by using EDX (energy dispersive X-ray analysis) unit attached to SEM model Quanta FEG 250. The specific surface area and mean pore size of the calcined bioactive glass powder were investigated by N_2 adsorption - isotherms desorption isotherms using high-speed gas sorption analyzer (NOVA 2000 series, Chromatic, UK) at 77 K. The Barrett–Emmett–Teller (BET) method was used to estimate the specific surface area.

III. RESULTS AND DISCUSSION

X-ray diffraction (XRD) pattern of the prepared bioactive glass powder after calcination at 650 ^{0}C for 2 h is given in Fig. 1. The obtained XRD chart shows the lack of any peaks exhibiting only abroad hump between 20^0 and 40^0 (2θ) which is indicating of the amorphicity of the structure of the prepared bioactive glass.

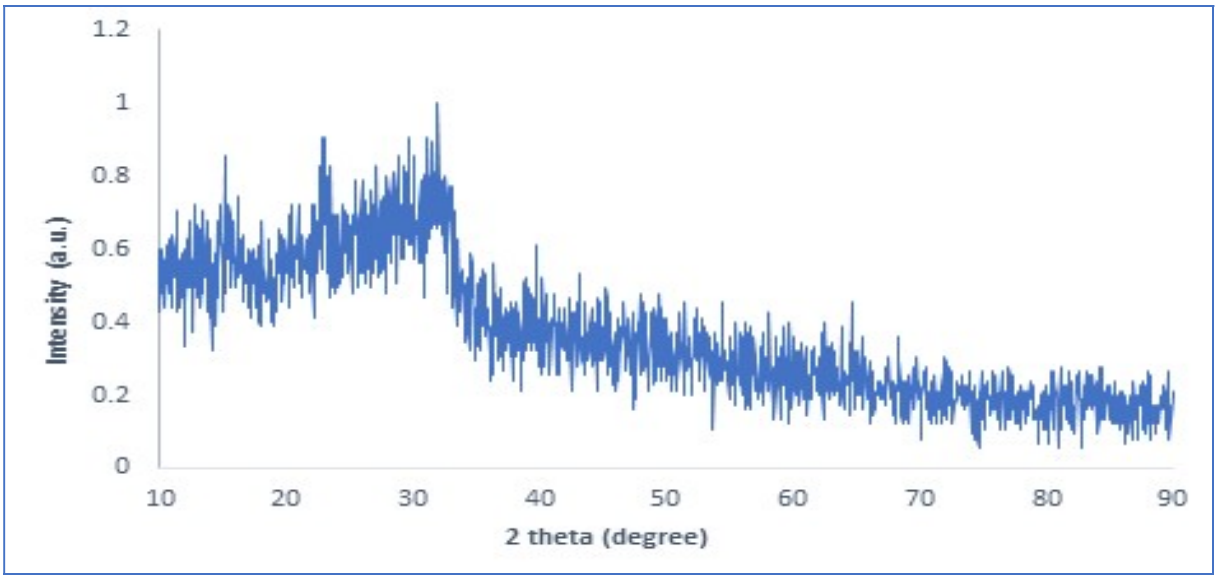

Figure 1. XRD pattern of the bioactive glass powder

Fig. 2. shows TEM image of the prepared glass powder calcined at 650 ^{0}C for 2 h. As demonstrated in this image, there are agglomerated particles. These particles have rod like to spherical features. As seen from image the measured size range of these particles was significantly less than 100 nm. Therefore, TEM analysis confirms that the prepared BG particles were in the nonorange and our goal in preparing the samples in nano range is achieved.

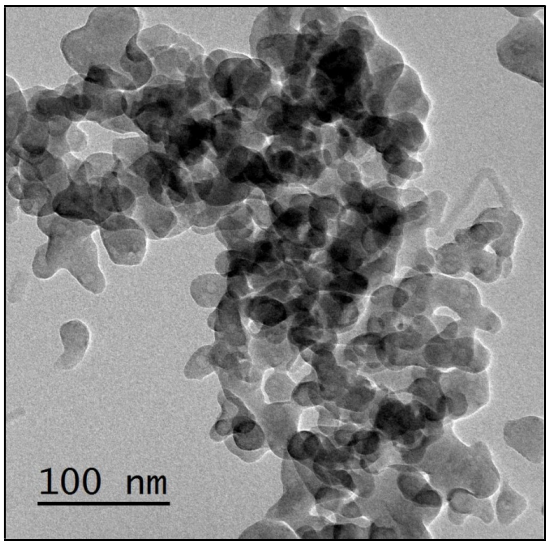

Figure 2. TEM analysis of calcined glass powder at 650 ^{0}C for 2 h.

Fig. 3. shows the infrared spectra of the calcined bioactive glass powder before and after immersion in SBF for 14 days. From the analysis of Fig. 3a. it can be easily seen that the unsoaked and soaked powders have distinguished peaks of silicate glass. Where, the peak which at nearly 460 cm^{-1} is attributed to a bending mode of Si–O –Si [6, 23]. Moreover, the band around 770 cm^{-1} and that a broad one around 1020 cm^{-1} are assigned to symmetric and asymmetric stretching vibrations of Si–O–Si respectively [6, 23]. Whereas, the peak around 600 cm^{-1} is corresponding to O–P–O phosphate bending absorption [24, 25]. The band at 1400 cm^{-1} is associated with carbonate group absorption. The peak at around 1600 cm^{-1} is corresponding to hydroxyl bending mode and a broad band around 3400 cm^{-1} is assigned to hydroxyl symmetric stretching mode due to tending of silicate glass to absorb moisture [26-28].

Fig. 3b. demonstrates the infrared spectra of sample after immersion in SBF for 14 days. As shown in the figure the new shoulder appears at about 880 cm^{-1} may be attributed to C−O stretching in carbonate groups which joining into the Ca−P layer for HCA formation [29]. Also, it shows the increasement of phosphate and hydroxyl intensities which also indicates the formation of hydroxycarbonate apatite (HCA) layer on the surface of sample after soaking in SBF.

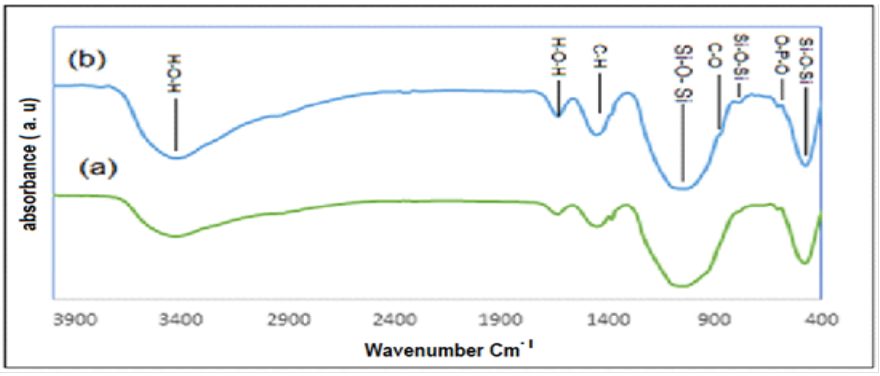

Figure 3. FTIR spectra for glass powder (a) before soaking in SBF, (b) after soaking in SBF.

Texture of calcined glass powder was analyzed by nitrogen adsorption and desorption isotherm technique as shown in Fig. 4. According to IUPAC classification, isotherm for the sample is of type IV and has H1 hysteresis loop [24, 30]. This means that the prepared glass powder is mesoporous and approximately cylindrical in shape. BET surface area, total pore volume and mean pore diameter of the sample are 54 m^2/g, 0.15 cm^3/g and 11.51 nm respectively which are determined from N_2 adsorption. The porous property of the prepared glass came from the way of gel formation during the preparation [12]. The presence of mesoporous texture makes the prepared glass more bioactive [29]. Fig. 4b. gives the curve of adsorption and desorption pore size distribution. This curve demonstrates a wide-ranging pore size distribution and approves the pores are in the mesopore scale. The porous property of the prepared glass came from the way of gel formation during the preparation [12]. The presence of mesoporous texture makes the prepared glass with a higher specific surface area and more bioactive [15, 29].

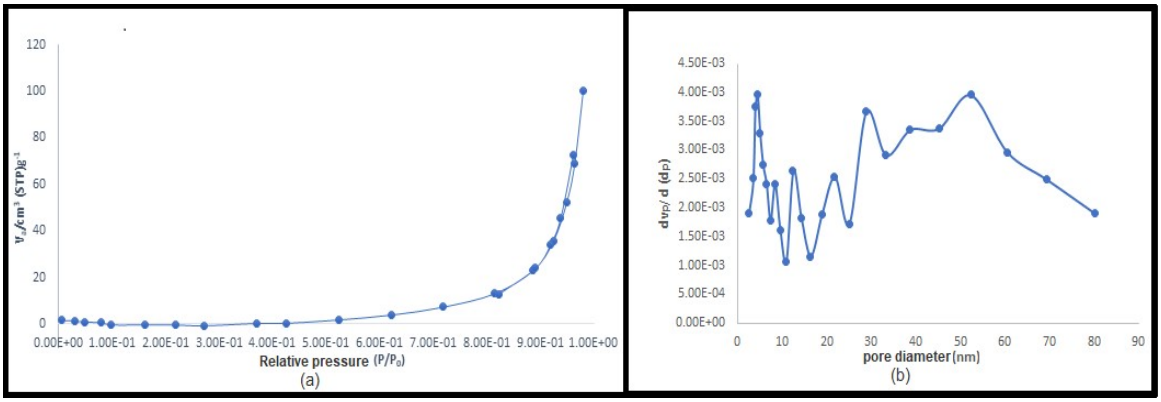

Figure 4. (a) Nitrogen adsorption and desorption isotherm of calcined glass powder, (b) the corresponding curve of adsorption and desorption pore size distribution.

Scanning electron microscopy (SEM) of the calcined bioactive glass disk (5 mm diameter and 2 mm thickness) before and after immersion in SBF for 14 days are given in Fig. 5. There is significant difference in the morphology of the surface of sample before and after soaking. The surface of unsoaked sample is nearly homogenous as seen in Fig. 5a. After soaking the sample surface is covered with HCA particles layer as shown in Fig. 5b.

EDX technique also confirms the formation of this new layer on the surface of the sample. EDX analysis was done to give the elemental composition of sample and to show the formation or not of an apatite-like phase on the sample surface after soaking them in SBF. Fig. 6a. illustrates EDX analysis of prepared glass disk before immersion in SBF. As shown in the figure the presence of Si, Ca, O_2 and P elements on the surface as any silicate bioactive glass. No

presence of any impurities peaks which confirming the high purity and accuracy during the sample preparation. Fig. 6b. shows EDX analysis of prepared bioactive glass disk after immersion them for 14 days in SBF. As given in the figure there is strong change in elemental concentration. The intensity of Si peaks in the specimen is strongly reduced. Appearance of Si peak represents silica gel due to the interaction process stage between SBF and glass sample to form HCA according to description of Hench [7]. While, the intensities of P and Ca peaks increase and become the main elements on the surface of prepared glass. It confirms the formation of HCA layer on sample surface. Additionally, the ratio of Ca to P is nearly identical to that of stoichiometric HCA [24, 31] which ensuring the formation of HCA layer. It guarantees the good bioactivity of prepared glass sample. EDX results confirms the formation of this new layer on the surface of the sample in consistent with the obtained data from SEM.

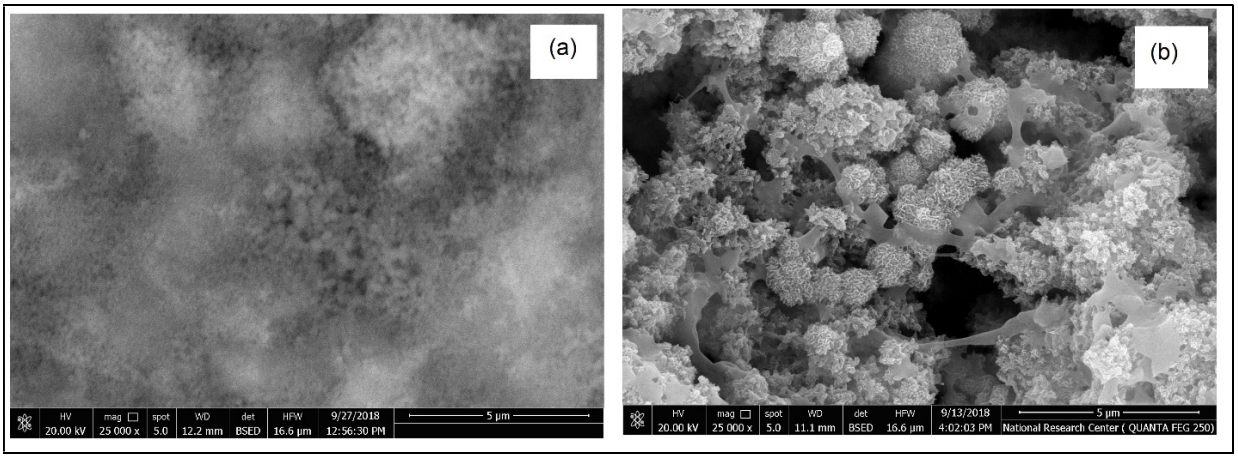

Figure 5. SEM images of bioactive glass sample (a) before soaking in SBF, (b) after soaking in SBF.

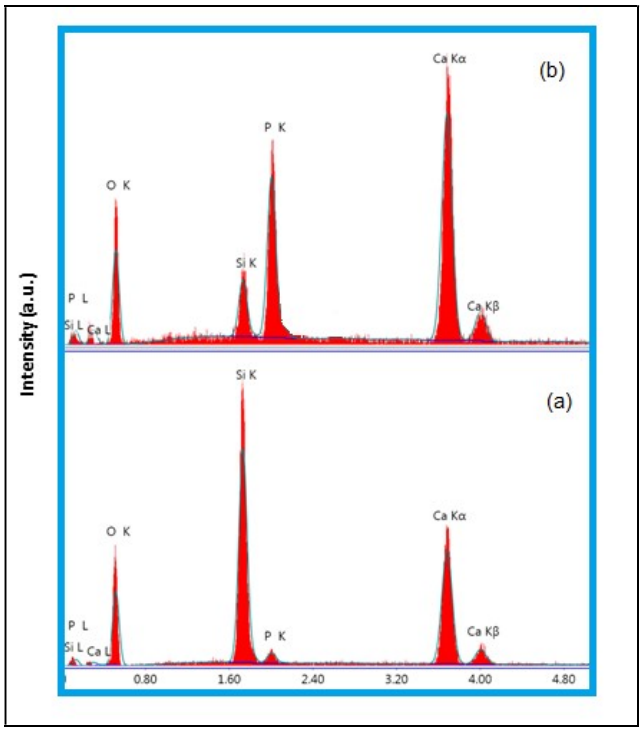

Figure 6. EDX analysis of bioactive glass sample (a) before soaking in SBF, (b) after soaking in SBF.

IV.CONCLUSION

Nanostructured bioactive glass was successfully prepared by sol-gel method. The results show that glass has internal disorder and amorphous nature after calcination at 650 ^{0}C. Texture analyses shows high surface area and porosity of prepared powder. SEM, EDX and FTIR results confirm the hydroxycarbonate apatite (HCA) layer formation on the surface of the sample upon soaking in SBF, indicating bioactive response of the prepared glass powder.

REFERENCES

[1] Alonso, L. M., García-Menocal, J. Á. D., García-Vallés, M., Manent, S. M., Balmayor, E. R., & van Griensven, M. "Exploring the use of silica sands and calcite from natural deposits to prepare bioactive glasses: Paper presented at the "VII International Congress of Biomaterials, BIOMAT'18", 14–16 March 2018, Havana, Cuba." International Journal of Materials Research (2018).

[2] Naseri, S., Lepry, W. C., & Nazhat, S. N. "Bioactive glasses in wound healing: hope or hype?." Journal of Materials Chemistry B 5.31 (2017): 6167-6174.

[3] Yu, H., Peng, J., Xu, Y., Chang, J., & Li, H. "Bioglass activated skin tissue engineering constructs for wound healing." ACS applied materials & interfaces 8.1 (2015): 703-715.

[4] Hench, L. L., Splinter, R. J., Allen, W. C., & Greenlee, T. K."Bonding mechanisms at the interface of ceramic prosthetic materials." Journal of biomedical materials research 5.6 (1971): 117-141

[5] Ohtsuki, C., Kokubo, T., & Yamamuro, T. "Mechanism of apatite formation on CaOSiO2P2O5 glasses in a simulated body fluid." Journal of Non-Crystalline Solids 143 (1992): 84-92.

[6] Arcos, D., Greenspan, D. C., & Vallet-Regi, M. "Influence of the Stabilization Temperature on Textural and Structural Features and Ion Release in SiO2− CaO− P2O5 Sol− Gel Glasses." Chemistry of Materials 14.4 (2002): 1515-1522.

[7] Hench, L. L., & Andersson, Ö. "Bioactive glasses." An introduction to bioceramics (1993): 41-62.

[8] Hench, L. L. "(ii) The challenge of orthopaedic materials." Current orthopaedics 14.1 (2000): 7-15.

[9] Wilson, J., & Low, S. B."Bioactive ceramics for periodontal treatment: comparative studies in the Patus monkey." Journal of Applied Biomaterials 3.2 (1992): 123-129.

[10] Vallet‐Regí, M., Ragel, C. V., & Salinas, A. J. " European Journal of Inorganic Chemistry 2003.6 (2003): 1029-1042.

[11] Hench, L. L. "Bioactive materials: the potential for tissue regeneration." Journal of Biomedical Materials Research: An Official Journal of The Society for Biomaterials, The Japanese Society for Biomaterials, and the Australian Society for Biomaterials 41.4 (1998): 511-518.

[12] Sepulveda, P., Jones, J. R., & Hench, L. L. "Characterization of melt‐derived 45S5 and sol‐gel−derived 58S bioactive glasses." Journal of Biomedical Materials Research: An Official Journal of The Society for Biomaterials, The Japanese Society for Biomaterials, and The Australian Society for Biomaterials and the Korean Society for Biomaterials 58.6 (2001): 734-740.

[13] Polini, A., Bai, H., & Tomsia, A. P. "Dental applications of nanostructured bioactive glass and its composites." Wiley Interdisciplinary Reviews: Nanomedicine and Nanobiotechnology 5.4 (2013): 399-410.

[14] Li, R., Clark, A. E., & Hench, L. L. "An investigation of bioactive glass powders by sol‐gel processing." Journal of Applied Biomaterials 2.4 (1991): 231-239.

[15] Vichery, C., & Nedelec, J. M. "Bioactive glass nanoparticles: from synthesis to materials design for biomedical applications." Materials 9.4 (2016): 288.

[16] Hench, L. L., & West, J. K. "The sol-gel process." Chemical reviews 90.1 (1990): 33-72.

[17] Nandi, S. K., Kundu, B., & Datta, S. "Development and applications of varieties of bioactive glass compositions in dental surgery, third generation tissue engineering, orthopaedic surgery and as drug delivery system." Biomaterials Applications for Nanomedicine. InTech, 2011.

[18] Erol‐Taygun, M., Zheng, K., & Boccaccini, A. R. "Nanoscale bioactive glasses in medical applications." International Journal of Applied Glass Science 4.2 (2013): 136-148.

[19] Yan, X., Yu, C., Zhou, X., Tang, J., & Zhao, D. "Highly ordered mesoporous bioactive glasses with superior in vitro bone‐forming bioactivities." Angewandte Chemie International Edition 43.44 (2004): 5980-5984.

[20] El-Kady, A. M., Ali, A. F., & Farag, M. M. "Development, characterization, and in vitro bioactivity studies of sol–gel bioactive glass/poly (l-lactide) nanocomposite scaffolds." Materials Science and Engineering: C 30.1 (2010): 120-131.

[21] Xia, W., & Chang, J. "Preparation and characterization of nano-bioactive-glasses (NBG) by a quick alkali-mediated sol–gel method." Materials letters 61.14-15 (2007): 3251-3253.04.

[22] Tadashi, K., Hyun-Min, K., Masakazu, K., Hiroaki, T., Toshiki, M., Masaki, U., & Takashi, N. "Nucleation and growth of apatite on amorphous phases in simulated body fluid." International Symposium on Crystallization in Glasses and Liquids (2000).

[23] Pereira, M. M., Clark, A. E., & Hench, L. L. "Calcium phosphate formation on sol‐gel‐derived bioactive glasses in vitro." Journal of Biomedical Materials Research 28.6 (1994): 693-698.

[24] Goh, Y. F., Alshemary, A. Z., Akram, M., Kadir, M. R. A., & Hussain, R. "In-vitro characterization of antibacterial bioactive glass containing ceria." Ceramics International 40.1 (2014): 729-737.

[25] Aguiar, H., Solla, E.L., Serra, J., González, P., León, B., Almeida, N., Cachinho, S., Davim, E.J.C., Correia, R., Oliveira, J.M. & Fernandes, M.H.V. "Orthophosphate nanostructures in SiO2–P2O5–CaO–Na2O–MgO bioactive glasses." Journal of Non-Crystalline Solids 354.34 (2008): 4075-4080.

[26] Adams, L. A., Essien, E. R., Shaibu, R. O., & Oki, A. "Sol-gel synthesis of SiO2-CaO-Na2O-P2O5 bioactive glass ceramic from sodium metasilicate." New Journal of Glass and Ceramics 3.01 (2013): 11.

[27] Siqueira, R. L., Peitl, O., & Zanotto, E. D. "Gel-derived SiO2–CaO–Na2O–P2O5 bioactive powders: synthesis and in vitro bioactivity." Materials Science and Engineering: C 31.5 (2011): 983-991.

[28] Weng, J., Liu, Q., Wolke, J. G. C., Zhang, X., & Groot, K. D. "Formation and Characteristics of the Apatite Layer on Plasma-Sprayed Hydroxyapatite Coating in Simulated Body Fluid," Biomaterials 18. 15 (1997): 1027-1035.

[29] Sepulveda, P., Jones, J. R., & Hench, L. L. "In vitro dissolution of melt‐derived 45S5 and sol‐gel derived 58S bioactive glasses." Journal of Biomedical Materials Research: An Official Journal of The Society for Biomaterials, The Japanese Society for Biomaterials, and The Australian Society for Biomaterials and the Korean Society for Biomaterials 61.2 (2002): 301-311.

[30] Sing, K. S. "Reporting physisorption data for gas/solid systems with special reference to the determination of surface area and porosity (Recommendations 1984)." Pure and applied chemistry 57.4 (1985): 603-619.

[31] Singh, R. K., & Srinivasan, A. "Apatite-forming ability and magnetic properties of glass-ceramics containing zinc ferrite and calcium sodium phosphate phases." Materials Science and Engineering: C 30.8 (2010): 1100-1106.